Journal of The
Electrochemical Society

Thermally Stable Electrolyte for Lithium-Ion Batteries

To cite this article: Larissa Kiefer *et al* 2025 *J. Electrochem. Soc.* **172** 120505

Journal of The Electrochemical Society, 2025 **172** 120505

Thermally Stable Electrolyte for Lithium-Ion Batteries

Larissa Kiefer,[1,z] Marco Ströbel,[1] Philipp Finster,[2] Carlos Ziebert,[2] and Kai Peter Birke[1]

[1] *University of Stuttgart, Institute for Photovoltaics, Electrical Energy Storage Systems, Pfaffenwaldring 47, 70569 Stuttgart, Germany*
[2] *Karlsruhe Institute of Technology (KIT), Institute for Applied Materials-Applied Materials Physics (IAM-AWP), Kaiserstraße 12, 76131 Karlsruhe, Germany*

The demand for safer, thermally stable lithium-ion batteries (LIBs) has driven the search for advanced electrolyte systems. This study introduces an electrolyte based on propylene glycol diacetate (PGDA) to improve thermal safety and stability. The optimized PGDA-based solvent mixture increases the flash point to 100 °C, which is approximately 63 K higher than that of the reference electrolyte LP40 (1 M $LiPF_6$ in EC:DEC 1:1 wt). While the flash point is primarily determined by the solvent composition, the onset of exothermic reactions depends on the conducting salt. Replacing lithium hexafluorophosphate ($LiPF_6$) with lithium bis(oxalato) borate (LiBOB) significantly improves thermal stability, cycling performance, and safety, as cells with LiBOB retain over 97% of their capacity after 100 cycles at 40 °C at C-rates up to 1C. Thermal abuse tests up to 300 °C exhibit no exothermic reactions, thereby preventing dangerous thermal runaways. These findings underscore the potential of PGDA-based electrolytes, especially when paired with LiBOB, for safer and more robust LIB applications.
 [DOI: 10.1149/1945-7111/ae235d]

Manuscript submitted September 4, 2025; revised manuscript received November 12, 2025. Published December 3, 2025.

Since the commercialization of the lithium-ion battery (LIB) by Sony in 1991, it has undergone continuous development. The energy density, power density, and longevity have been significantly improved, establishing LIBs as the leading technology for storing electrical energy, particularly in mobile applications.[1–3]

However, the electrolyte has seen little advancement during this period. In most cases, it still consists of highly flammable and volatile solvents, lithium-conducting salts, and various additives.[4,5] As the cell temperature increases, the internal pressure of LIBs with these electrolytes also rises. Above 80 °C, the passivation layer on the graphite electrode (solid electrolyte interphase, SEI) decomposes and reforms, with both processes being exothermic, leading to the formation of even more flammable gases.[6,7] The resulting high gas pressure can damage the cell, allowing the flammable gas to escape and ignite. At approximately 170 °C, the worst-case scenario occurs, where these reactions lead to significantly accelerated self-heating of the cell, ultimately resulting in thermal runaway.[8,9] During this process, the battery ignites due to excessive heat generation, reaching temperatures of up to 1000 °C and releasing toxic fumes.[10–13] Therefore, the further development of the electrolyte is a key requirement for enhancing the safety of LIBs.

There are various approaches to reducing the flammability of the electrolyte or replacing it with non-flammable substances. These approaches include the use of ionic liquids,[14,15] polymer electrolytes,[16,17] or solid-state electrolytes.[18,19] However, all of these approaches are still in the research stage and generally exhibit significantly lower conductivity than conventional liquid electrolytes.

The aim of the present study is to improve the thermal safety of liquid electrolytes. For this purpose, we present the solvent propylene glycol diacetate (PGDA) in combination with ethylene carbonate (EC), propylene carbonate (PC), and the conducting salt lithium bis(oxalato) borate (LiBOB) as a new liquid electrolyte for NCM/graphite LIBs. The flash point of the new PGDA-based electrolyte is around 100 °C, which is significantly higher than that of state-of-the-art electrolytes (approximately 37 °C[20]). At a C-rate of 1.5C, 95% of the usable capacity can still be discharged. Particularly outstanding is the fact that in thermal abuse tests, where the cells are heated up to 300 °C, no exothermic reactions—and thus no signs of thermal runaway—are observed. As a result, the presented electrolyte can significantly improve the thermal safety of LIBs while maintaining high conductivity.

Methods

Materials.—Propylene glycol diacetate (PGDA, purity > 99.7%, from Sigma Aldrich, Darmstadt, Germany) was first introduced into a glove box with an argon atmosphere and a moisture content of less than 0.5 ppm. Subsequently, it was dried overnight by adding a molecular sieve (mesh size ≈ 0.3 nm). The chemical structure of PGDA is illustrated in Fig. 1. The solvents ethylene carbonate (EC, purity 99%, from Sigma Aldrich, Darmstadt, Germany), propylene carbonate (PC, purity > 99.7%, from Carl Roth, Karlsruhe, Germany) and ethyl methyl carbonate (EMC, purity > 99.9%, from Sigma Aldrich, Darmstadt, Germany) as well as the conducting salts lithium hexafluorophosphate ($LiPF_6$, from BASF, Ludwigshafen, Germany) and lithium bis(oxalato) borate (LiBOB, from Sigma Aldrich, Darmstadt, Germany) were opened in the glove box and used as received. Graphite electrodes with a capacity of 3 mAh/cm^2 (provided by Varta AG, Ellwangen, Germany) and lithium nickel manganese cobalt oxide electrodes with a capacity of 1.3 mAh/cm^2 (NCM 622, provided by Münster Electrochemical Energy Technology, Münster, Germany) were punched into 18 mm diameter coins and dried in a vacuum oven (B-585 from Buechi Labortechnik AG, Flawil, Switzerland, $p < 50$ mbar) for 16 hours at a temperature of $T = 120$ °C. The separator FS 2190 (from Freudenberg, Weinheim, Germany, thickness ≈200 μm) was punched into 21 mm diameter coins and dried under the same conditions. The electrolyte *Selectilyte LP40* (1 M $LiPF_6$ in EC:DEC 1:1 wt, from BASF, Ludwigshafen, Germany) was used for reference measurements.

Electrolyte preparation.—The electrolytes were mixed in a LABstar glove box from M. Braun Inertgas-Systeme (Garching, Germany) filled with argon, whereby the water and oxygen values were kept below 0.5 ppm. All tested electrolytes have a salt concentration of 1 M $LiPF_6$ respectively 0.6 M LiBOB. The solvents were added in different weight proportions and compositions (presented in Table I).

Cell assembly.—To assemble the cells, the polypropylene separator FS 2190 is first wetted on both sides with a total of $V = 120$ μl of the respective electrolyte. For the assembly of full

[z] E-mail: larissa.kiefer@ipv.uni-stuttgart.de

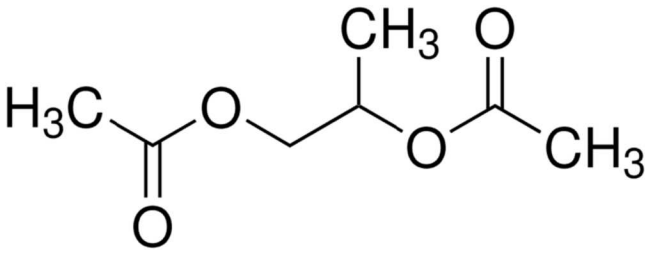

Figure 1. Structural formula of propylene glycol diacetate (PGDA).[21]

Table I. Melting point (T_{MP}), flash point (T_{FP}) and boiling point (T_{BP}) of PGDA,[21] EC,[22,23] PC[22,23] and EMC[22,24] and analyzed solvent mixtures by weight (wt).

	PGDA	EC	PC	EMC
T_{MP} (°C)	−70	36	−49	−53
T_{FP} (°C)	87	145	135	23
T_{BP} (°C)	191	248	242	107
	85%	15%	—	—
	70%	15%	15%	—
	60%	15%	25%	—
	50%	15%	35%	—
	65%	15%	15%	5%
	55%	15%	25%	5%
	45%	15%	35%	5%

cells, the NCM working electrode is then placed on one side and graphite as the counter electrode on the other side of the separator. The cells are then installed in PAT-Cell or ECC-Ref housings from EL-Cell (Hamburg, Germany) for electrochemical characterization and in CR2016 housings for calorimetry measurements.

Cell tests.—To characterize and optimize the cells with the new electrolyte, C-rate tests, aging tests and tests at various temperatures were carried out. All these measurements were performed on the CTS battery tester from BaSyTec (Asselfingen, Germany). The cells were kept in an IPP 110 climate chamber from Memmert (Schwabach, Germany) during the entire measurement to maintain the desired temperature. Before starting the actual measurement, all cells were formed by three cycles at C/10, followed by three formation cycles at C/5 CC charge and CC discharge. The lower voltage limit is 2.5 V, the upper voltage limit is 4.2 V.

Cyclic voltammetry (CV) measurements.—The cells for the CV measurements were set up with inert stainless steel electrodes serving as the working, counter, and reference electrodes. The electrochemical stability of the electrolytes was assessed using linear sweep voltammetry. These measurements were conducted with a Reference 3000 AE from Gamry (Warminster, PA, USA). The sampling rate was set at 0.5 mV/s, with potential limits ranging from −4.3 V to 4.3 V against stainless steel.

Flash point measurement.—The NPV Tech flash point tester from Normalab (Valliquerville, France) is used for determining the flash point of the electrolytes. The measurements conform to the ISO 3679 standard, which is a rapid equilibrium method in closed vessels. The device enables the determination of the flash point in a temperature range of −30 to 300 °C. An integrated barometer measures the air pressure at the time of the flash point determination, and the measured flash point is corrected to standard pressure. The required sample volume is 2 ml for measurements below 100 °C, while higher temperatures necessitate 4 ml of solvent for the measurement. The determination of the flash point is carried out in two steps. First, the approximate flash point is determined using the automatic mode. For this, the electrolyte is placed in the designated chamber and then heated with a defined gradient. At each full degree, the flammability is checked by an external ignition source. As soon as ignition is detected, the measurement ends automatically. For a precise flash point determination, a subsequent measurement is performed in manual mode according to ISO 3679. New electrolyte is placed in the sample chamber, brought to a specific temperature, and tested to see whether or not ignition occurs. The first measurement in manual mode is conducted at a temperature 2 degrees below the temperature determined in automatic mode. If there is no ignition, the measurement is repeated with new electrolyte and a temperature that is 1 degree higher than the previous test temperature. This process is repeated until a flash point is detected.

Conductivity measurements.—To determine the electrolyte conductivity, the electrolyte is filled into a Platinized HTCC Conductivity Cell from BioLogic (Seyssinet-Pariset, France) and connected to the Reference 3000 AE from Gamry (Warminster, PA, USA). To measure the conductivity as a function of temperature, the measuring cell is then placed in the water bath of the Proline RP 845 thermostat from Lauda (Lauda-Königshofen, Germany) and the resistance is measured at 1000 Hz in 5-degree increments from 5 to 60 °C. The conductivity is then determined from the measured resistances using the cell constant, which was previously determined with an electrical conductivity (EC) standard solution.

Thermal abuse test.—To perform thermal abuse experiments, the heat-wait-seek (HWS) test was employed following the methodology outlined in Ref. 25. For this purpose, the ES ARC device from Thermal Hazard Technology (Bletchley, UK) was utilized. This instrument possesses the sensitivity required to precisely monitor the thermal behavior of coin cells with capacities in the range of 5 mAh.[26,27] Since the individual coin cells had relatively low capacities, four cells were combined for each experiment, resulting in a cell stack with a capacity of approximately 8 mAh. The cells were taped together with a type E thermocouple placed at the center of the stack using heat-resistant tape provided by 3M Industrial Business (Neuss, Germany). During the measurements the stack was positioned centrally within the calorimeter to ensure even heat distribution. Before conducting the thermal abuse tests, the ARC device was calibrated according to the manufacturer's instructions, using coin cell dummies with comparable heat capacities and identical experimental conditions. After calibration, a drift test was performed to confirm the accuracy of the device.

The test comprises three distinct phases: heat, wait, and seek. In the initial heat phase, the temperature is raised from room temperature to 35 °C, while in all subsequent heat phases the temperature is increased by 5 K. The heat phase is followed by the wait phase, which allows thermal equilibrium to be established after each incremental temperature increase. The waiting period between successive heating steps was set to 20 minutes. During the seek phase, temperatures recorded by two thermocouples—one positioned near the heater and the other close to the sample—were compared. If a temperature difference is observed, the system determines the heating rate. When the rate surpasses a predefined limit of 0.02 °C/min, self-heating is identified, triggering a transition to a (quasi-) adiabatic state called exotherm mode. In this mode, heat exchange with the surroundings is minimized, enabling exothermic reactions within the cell to proceed. The cell's temperature then increases until either thermal runaway occurres or the reactants fueling the exothermic reaction are exhausted. Certain phenomena, such as venting or endothermic reactions, could temporarily interrupt the self-heating process and cause the system to continue with another heating step until exothermic activity resumes or the cell enters into thermal runaway. More details on this procedure can be found in Ref. 28. To prevent damage to the calorimeter, the test was concluded at 300 °C if thermal runaway had not occurred by this

point, under the assumption that the cell would not enter runaway thereafter.

Results and Discussion

In the following, PGDA is presented as a non-toxic solvent in the electrolyte of lithium-ion cells, which has the potential to improve the thermal safety of lithium-ion cells due to its physical properties. Furthermore, its low melting point offers advantages at low operating temperatures. The aim of this study is to develop an electrolyte that is preferably free of volatile linear carbonates and has an increased thermal stability.

Optimization of the solvent composition.—The solvents used for electrolyte optimization and their physical properties as well as the electrolyte mixtures tested are listed in Table I. The composition of the PGDA-based electrolyte was optimized using 1 M lithium hexafluorophosphate ($LiPF_6$) as the salt, along with the addition of ethylene carbonate (EC), propylene carbonate (PC), and ethyl methyl carbonate (EMC), whereby the proportion of EMC as a linear carbonate with a low flash point is limited to 5% and the EC content is kept constant at 15% for all cells. EC is essential for SEI formation in the electrolyte, but has a high melting point of 35 °C and is solid at room temperature; therefore, its content was limited to 15% to ensure proper performance at low temperatures. The purpose of the optimization was to enhance the electrolyte's performance by balancing the properties of the solvents, which influence viscosity, conductivity, and electrochemical stability. The various ratios of PGDA, EC, PC, and EMC were systematically tested to determine the most effective combination for improving the ionic conductivity and cycling stability.

The aging behavior of electrolytes with different solvent ratios was investigated using life cycle tests over 100 cycles at $T = 25$ °C. After formation, the cells were charged with C/2 constant current, constant voltage (CCCV) and discharged with 1C constant current (CC). Figure 2a shows the influence of the PC content. Proportions between 0 and 35% were tested. The best result was achieved with the mixture 1 M $LiPF_6$ in PGDA:PC:EC (60:25:15 wt). This cell had both the highest usable capacity and the lowest cyclic aging. After 100 cycles, the cell has a remaining capacity of 96.7%. The cell without PC achieves similar capacities during formation as the cells with PC. However, at the start of the cycling and thus when the C-rates are increased to C/2 during charging and to 1C during discharging, the usable capacity drops significantly. These results indicate that the addition of PC substantially promotes the electrochemical performance of the cell system.

The addition of 5% EMC can initially increase the usable capacity of the cells, but the degradation during cycling is significantly higher, so that the remaining capacity after 100 cycles is approx. 88% for all cells with EMC. The cells with EMC are shown in Fig. 2b.

Due to the higher aging observed in cells containing EMC and the fact that the addition of volatile EMC significantly reduces the flash point of the electrolyte, the EMC-free electrolyte 1 M $LiPF_6$ in PGDA:PC:EC (60:25:15 wt) is used for further investigations. To further improve the thermal stability of the electrolyte, tests were conducted using the same solvent mixture but with conducting salts known for their higher thermal stability, such as lithium bis (trifluoromethane sulfonyl)imide (LiTFSI), with a decomposition temperature of around 360 °C,[29] and LiBOB, with a decomposition temperature exceeding 300 °C.[30] In contrast, $LiPF_6$ decomposes above 55 °C.[29] However, LiTFSI appears to be incompatible with the PGDA:PC:EC solvent mixture, as cells with 1 M LiTFSI in PGDA:PC:EC (60:25:15 wt) exhibit significant capacity loss within the first 100 cycles. In the further course, the determined solvent mixture is also tested with the thermally stable conducting salt LiBOB. Here, 0.6 M was determined as the optimum concentration of the solution.

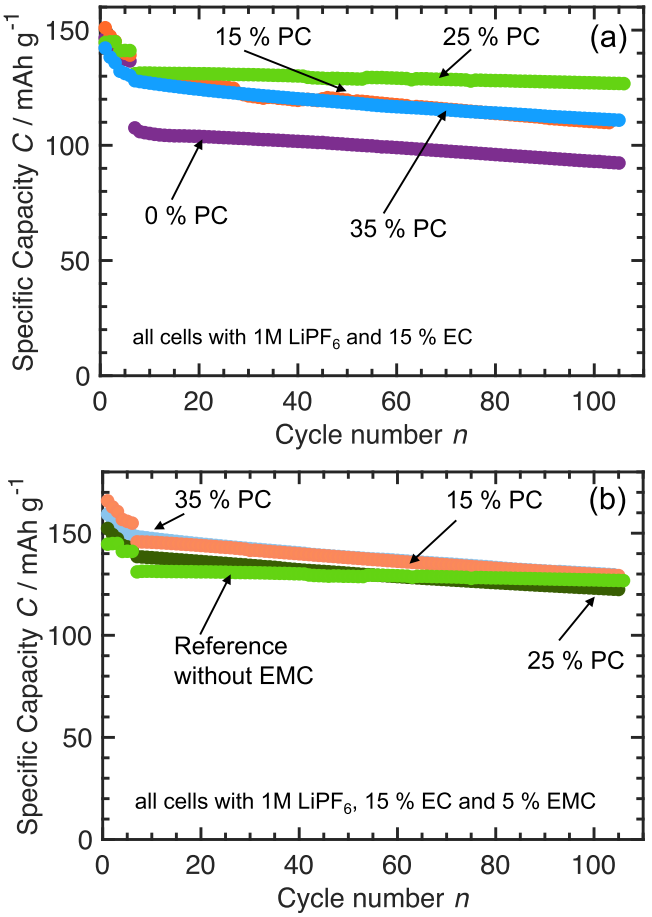

Figure 2. Specific discharge capacity of NCM/graphite cells with (a) 1 M $LiPF_6$ in PGDA:PC:EC with a constant amount of 15% EC and variable proportions of PGDA and PC and (b) 1 M $LiPF_6$ in PGDA:PC:EC:EMC with a constant amount of 15% EC and 5% EMC and variable proportions of PGDA and PC. The best cell without EMC (1 M $LiPF_6$ in PGDA:PC:EC (60:25:15 wt)) is also shown for better comparability. The first three cycles are formation cycles at C/10, followed by three formation cycles at C/5. After formation, the cells were charged with C/2 CCCV and discharged with 1C CC. The cell with the solvent mixture PGDA:PC:EC (60:25:15 wt) has the best aging behavior.

Life cycle performance at different temperatures.—Figure 3a presents the life cycle performance of the new electrolytes 1 M $LiPF_6$ in PGDA:PC:EC (60:25:15 wt) and 0.6 M LiBOB in PGDA:PC:EC (60:25:15 wt) compared to a cell with LP40 as the standard electrolyte at $T = 25$ °C. Initially, the usable capacity of the cells with the PGDA-based electrolytes is slightly lower than that of the cell with LP40, but the degradation rate of the LP40 cell is marginally higher. Overall, the performance of all three cells is quite comparable. After 92 cycles, the remaining capacity of the LP40 cell is 93.7% compared to the initial capacity after formation, while the cell with $LiPF_6$-PGDA has a remaining capacity of 97% and the LiBOB-PGDA cell a capacity of 97.8% after the same number of cycles.

Additionally, cycling tests with the new electrolytes were conducted at $T_2 = 10$ °C and $T_3 = 40$ °C. The results are presented in Fig. 3b. Due to the lower ionic conductivity at low temperatures and the increased risk of lithium plating, the C-rate at 10 °C is reduced to C/4 for CCCV charging and C/2 for CC discharging. A notable

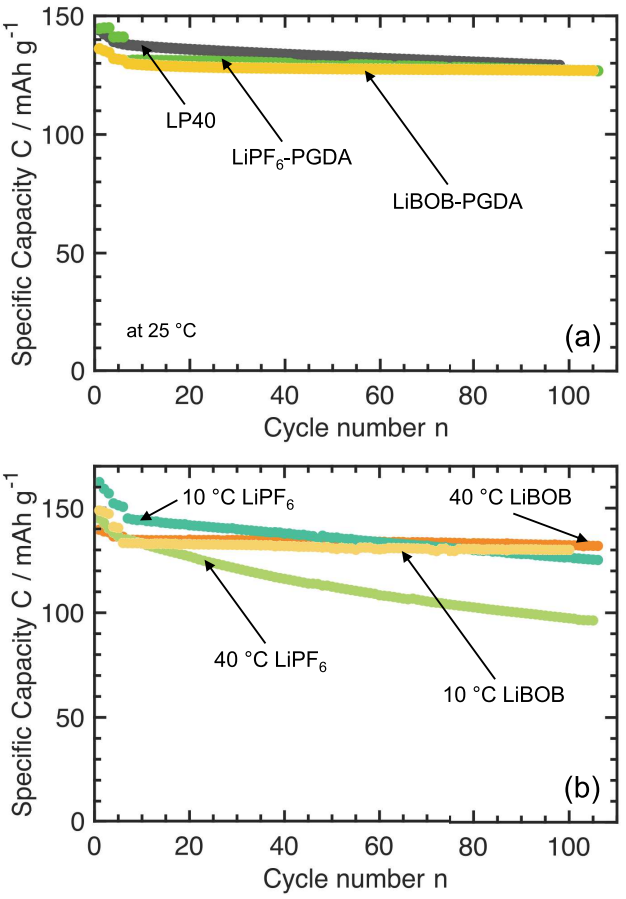

Figure 3. Specific discharge capacity of NCM/graphite cells with (a) 1 M $LiPF_6$ in PGDA:PC:EC ($LiPF_6$-PGDA), 0.6 M LiBOB in PGDA:PC:EC (LiBOB-PGDA) and the standard electrolyte LP40 at $T_1 = 25$ °C and (b) 1 M $LiPF_6$ in PGDA:PC:EC ($LiPF_6$) and 0.6 M LiBOB in PGDA:PC:EC (LiBOB) at $T_2 = 10$ °C and $T_3 = 40$ °C. The first three cycles are formation cycles at C/10, followed by three formation cycles at C/5. After formation, the cells were charged at 25 °C and 40 °C using a C/2 CCCV protocol and discharged with a 1C CC rate. At 10 °C, the cells were charged using a C/4 CCCV protocol and discharged with C/2 CC. Cells with LiBOB-based electrolyte show a significantly reduced capacity loss compared to cells with the $LiPF_6$-based electrolyte.

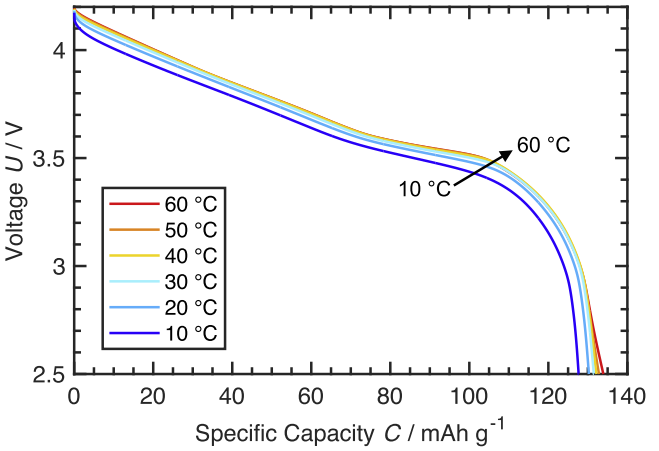

Figure 4. Voltage profiles of a NCM/graphite cell with 0.6 M LiBOB in PGDA:PC:EC (60:25:15 wt) at different temperatures and a C-rate of C/4. At a temperature of 10 °C, over 95% of the capacity can still be converted compared to the maximum extractable capacity, which is reached at a temperature of 60 °C.

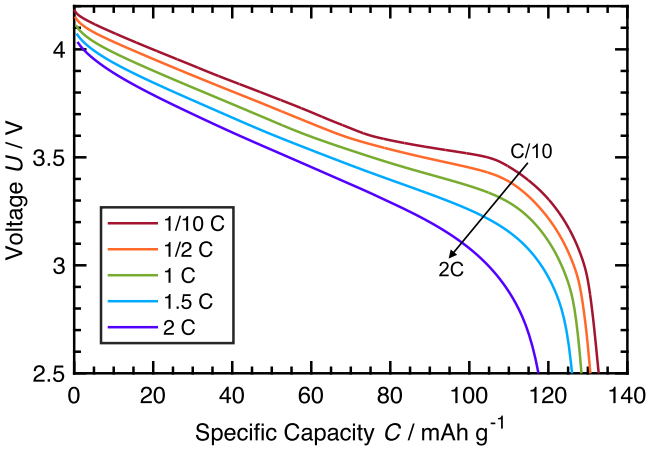

Figure 5. Voltage profiles and specific discharge capacity of a NCM/graphite cell with 0.6 M LiBOB in PGDA:PC:EC (60:25:15 wt) at $T = 25$ °C and different C-rates of C/10, C/2, 1C, 1.5C and 2C. Up to a C-rate of 1.5C, 95% of the capacity remains accessible. At higher C-rates, however, the transferable charge decreases significantly.

observation is the significantly stronger aging of cells with $LiPF_6$ in the electrolyte. After 94 cycles, the cells tested at 40 °C retain 72.2% of its initial capacity, while the cells at 10 °C retain 87.2% of its capacity. In contrast, cells utilizing LiBOB as the conducting salt demonstrate superior performance, retaining a capacity of at least 97.6% regardless of the temperature after the same number of cycles.

These results highlight the potential of LiBOB as a highly stable electrolyte system in combination with PGDA:PC:EC under varying thermal conditions. This stability is also evidenced by the voltage profiles and extractable discharge capacity, which exhibit minimal dependence on temperature across the tested range of 10 °C to 60 °C at a C-rate of C/4. As illustrated in Fig. 4, the extractable discharge capacity at 10 °C is slightly reduced compared to higher temperatures. This reduction can be attributed to the lower ionic conductivity of the electrolyte at lower temperatures. However, within the temperature window of 20 °C to 60 °C, the variations in both the extractable capacity and the voltage profiles are negligible, reflecting the robustness of the electrolyte composition in maintaining performance stability over a broad temperature range.

C-rate tests of the LiBOB-PGDA electrolyte.—In order to determine the usable capacity as a function of the C-rate, the cells were discharged at C-rates of C/10, C/2, 1C, 1.5C and 2C. After each discharge step, the cells were recharged at a constant C-rate of C/6. Figure 5 shows the voltage profiles and specific discharge capacity of the cell with 0.6 M LiBOB in PGDA:PC:EC (60:25:15 wt) at the different C-rates. Up to a C-rate of 1.5C, 95% of the capacity, relative to the capacity at C/10, can be used. With further increasing C-rates, the capacity drop is significantly higher.

Flash point and conductivity.—One objective of developing the new electrolyte is to significantly increase the flash point compared to conventional electrolytes. LP40 is used as the reference electrolyte, with a flash point of approximately $T_{FP} \approx 37$ °C, which can be critical for safety. During operation, the cell can easily reach temperatures exceeding 50 °C, leading to the release of flammable gases in the event of mechanical damage.

The flash point of the new solvent mixture PGDA:PC:EC (60:25:15 wt), measured according to ISO 3679, is $T_{FP} = 101 \pm 2$ °C. When combined with 0.6 M LiBOB, the flash point is $T_{FP} = 100 \pm 2$ °C, and with 1 M $LiPF_6$, it is $T_{FP} = 108 \pm 2$ °C. Therefore, the flash point of the PGDA-based electrolyte is about 63 K higher than that of LP40. This is particularly relevant considering that the typical permissible operating temperature for lithium-ion cells is around 60 °C, with the (SEI) beginning to decompose at approximately 80 °C.[3] Consequently, the

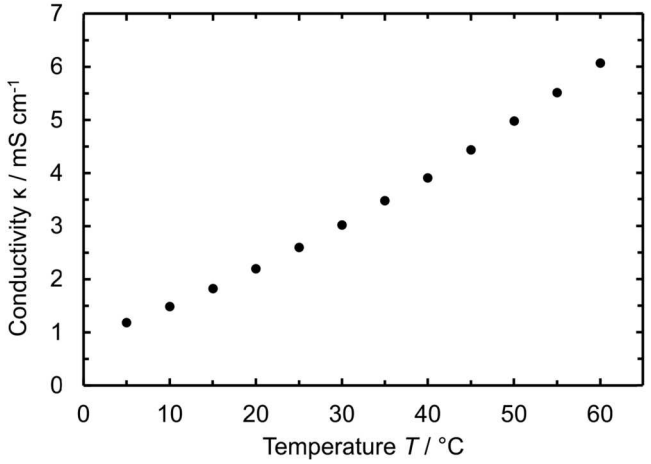

Figure 6. Conductivity of the 0.6 M LiBOB in PGDA:PC:EC (60:25:15 wt) electrolyte in the temperature range from 5 °C to 60 °C. The conductivity of the new electrolyte is 2 to 3 times lower than that of the reference electrolyte LP40 and therefore still within the same order of magnitude.

flash point of the PGDA-based electrolyte remains well above typical operating conditions, enhancing the cell's thermal safety.

Figure 6 shows the conductivity of the electrolyte 0.6 M LiBOB in PGDA:PC:EC (60:25:15 wt) at temperatures ranging from 5 °C to 60 °C. At $T = 25$ °C, the electrolyte has a conductivity of approximately 2.6 mS/cm. In comparison, LP40 has a conductivity of about 7.6 mS/cm at the same temperature. Therefore, the conductivity of LP40 at $T = 25$ °C is approximately 3 times higher than that of the new electrolyte. Thus, the conductivity of the new electrolyte is indeed lower; however, it is in the same order of magnitude as the conductivity of LP40, which allows C-rates of up to 1C without any issues.

Cyclic voltammetry.—To investigate the electrochemical stability window of 0.6 M LiBOB in PGDA:PC:EC (60:25:15 wt), CV measurements are conducted. The potential window from −4.3 to + 4.3 V against stainless steel is considered. Figure 7a shows the measured current density versus potential. For comparison, the measurement with LP40 is shown in Fig. 7b. The detected current density of the PGDA electrolyte is in the range between −6.7 and + 3.7 μA/cm^2 throughout the entire potential window and is therefore in the same order of magnitude as the current density observed with LP40, which reaches peak values of −7.8 and +5 μA/cm^2. Compared to LP40, the PGDA electrolyte thus exhibits a comparable electrochemical stability within the potential window relevant for lithium-ion cells.

Thermal abuse test.—To assess the thermal safety of the developed electrolytes, heat-wait-seek (HWS) testing was performed using an accelerating rate calorimeter. Coin cells with an NCM/graphite chemistry were assembled, employing the novel electrolytes 1 M $LiPF_6$ in PGDA:PC:EC (60:25:15 wt) and 0.6 M LiBOB in PGDA:PC:EC (60:25:15 wt) alongside the reference electrolyte LP40. After cell formation, the cells were charged to a 100% state of charge (SoC). The HWS test involved incrementally increasing the temperature in 5 °C steps. After each heating step, a waiting phase of 20 minutes was conducted to observe whether the cell exhibited self-heating without any external energy input. Such behavior would indicate the occurrence of exothermic reactions within the cell. The measurement results are presented in Fig. 8. The cells with $LiPF_6$ in the electrolyte (see Fig. 8a LP40 and 8b 1 M $LiPF_6$ in PGDA:PC:EC (60:25:15 wt)) show a self-sustained temperature increase starting at approximately 170 °C, regardless of the solvents used. This indicates exothermic reactions that could

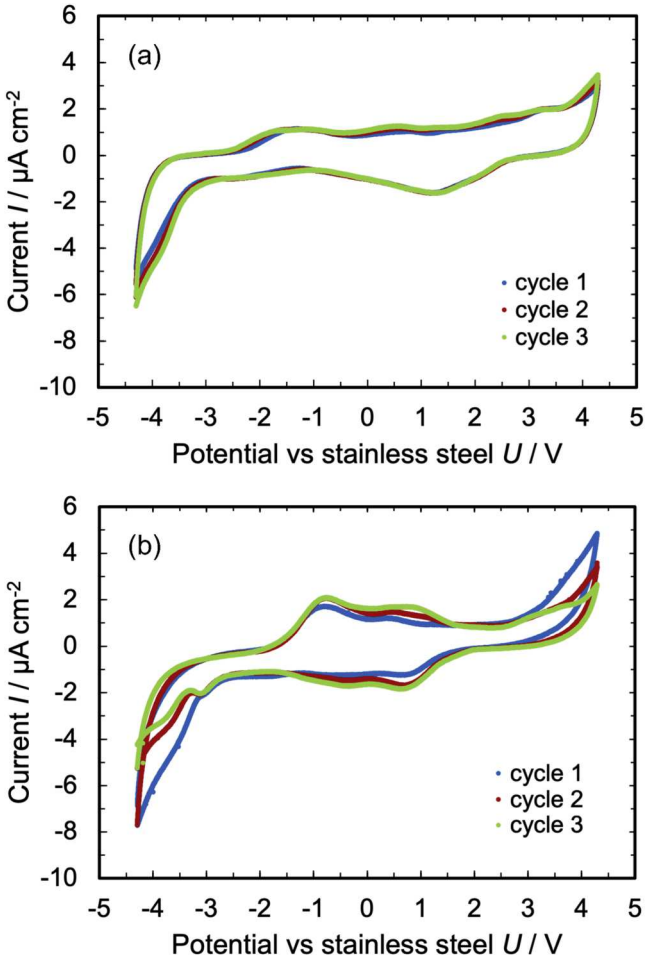

Figure 7. Electrochemical stability window of (a) 0.6 M LiBOB in PGDA:PC:EC (60:25:15 wt) and (b) LP40. The working and counter electrode is stainless steel and the scan rate is 0.5 mV/s. In the relevant potential window, the measured currents for both electrolytes are similar, indicating that the stability of the two electrolytes is comparable.

potentially lead to thermal runaway of the cell. The novel electrolyte based on $LiPF_6$ additionally exhibits exothermic reactions at around 90 °C, which could be attributed to the decomposition of the solid electrolyte interphase (SEI). In contrast, the new LiBOB-PGDA-based electrolyte shown in Fig. 8c displays no exothermic reactions. Consequently, the newly developed electrolyte is thermally stable up to at least 300 °C, thereby contributing to the prevention of thermal runaway in lithium-ion cells.

Conclusions

This study presents a novel electrolyte system based on the solvent PGDA in combination with the lithium salt LiBOB, optimized for use in NCM/graphite lithium-ion cells. By eliminating volatile linear carbonates and leveraging the physical properties of PGDA, the electrolyte demonstrates significantly enhanced thermal safety and stability compared to the reference electrolyte LP40. Specifically, the optimized solvent mixture of PGDA:PC:EC (60:25:15 wt) has a flash point of approximately 100 °C, representing a significant increase of about 63 K compared to LP40. The results also show that the flash point of the electrolyte is primarily determined by the solvent mixture, with the conducting salt having only a minor influence.

In contrast, the onset of exothermic reactions during thermal abuse testing was found to be largely dependent on the conducting

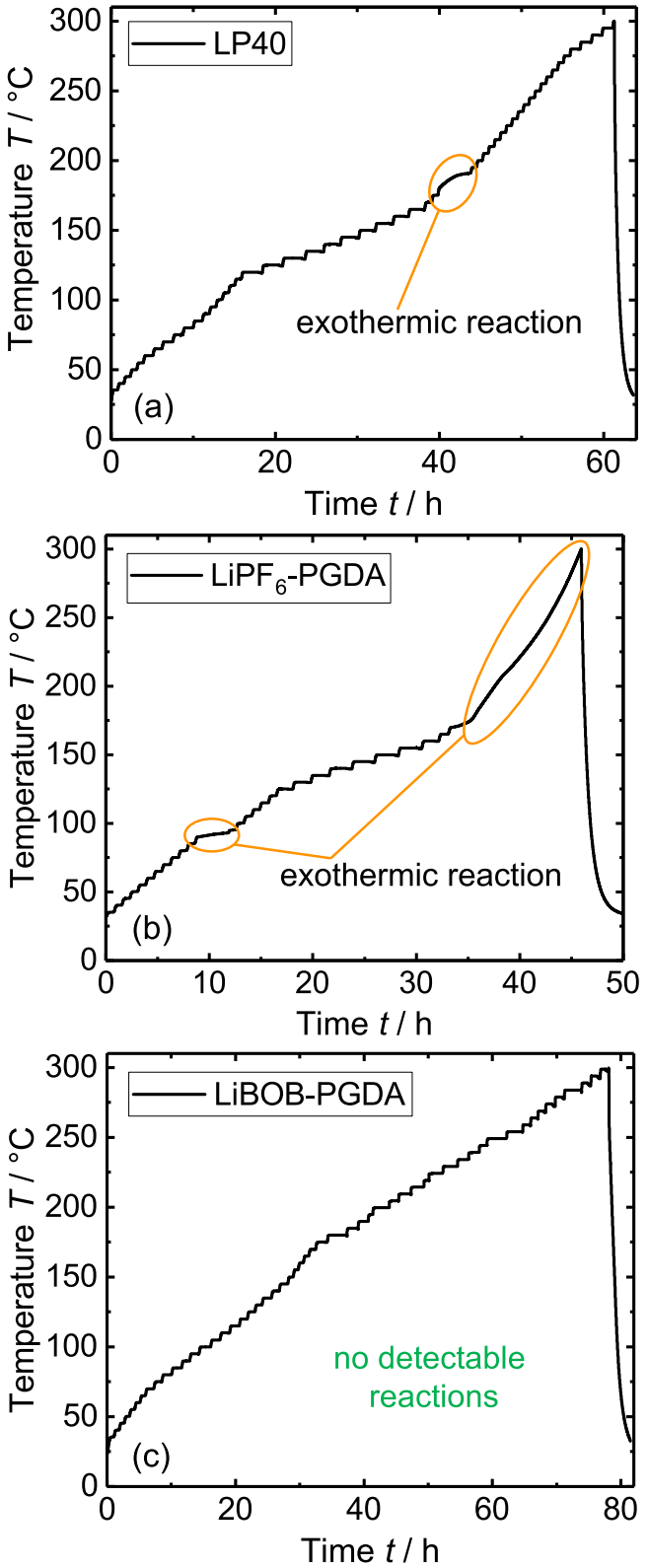

Figure 8. Data of the thermal abuse tests of NCM/graphite cells with (a) LP40 (b) 1 M $LiPF_6$ in PGDA:PC:EC (60:25:15 wt) and (c) 0.6 M LiBOB in PGDA:PC:EC (60:25:15 wt). The cells with $LiPF_6$ in the electrolyte show a self-sustained temperature increase starting at approximately 170 °C, indicating exothermic reactions. In the cell with the novel $LiPF_6$-PGDA electrolyte, additional exothermic reactions occur at around 90 °C, whereas no exothermic reactions are observed in the cell with the new LiBOB-PGDA-based electrolyte. Thus, the LiBOB-PGDA electrolyte enables the production of thermally safe cells.

salt rather than the solvent composition. Cells with PGDA:PC:EC (60:25:15 wt) and $LiPF_6$ as the conducting salt exhibited rapid capacity degradation at elevated temperatures and triggered exothermic reactions at thresholds similar to those of the conventional LP40 electrolyte. However, replacing $LiPF_6$ with 0.6 M LiBOB led to significant improvements in both thermal stability and cycling performance. Cells using LiBOB retained over 97% of their capacity after 100 cycles, even at 40 °C, and showed no exothermic reactions during thermal abuse tests conducted up to 300 °C. This highlights the exceptional thermal stability of the newly developed electrolyte, as it remains stable up to 300 °C without triggering thermal runaway. In contrast, commercial lithium-ion cells using conventional electrolytes typically show the onset of exothermic reactions at approximately 90 °C. Once the temperature reaches around 150 °C, the point of no return is reached, at which the cell is highly likely to enter thermal runaway.[31] The results demonstrate that the combination of a thermally stable conducting salt and a solvent mixture with a high flash point is necessary to enhance the thermal stability and safety of lithium-ion cells and effectively suppress thermal runaway.

Although the ionic conductivity of the PGDA-based electrolyte is lower than that of LP40, it is sufficient to support C-rates up to 1C, ensuring reliable operation. Cyclic voltammetry measurements demonstrated a similar electrochemical stability for the new 0.6 M LiBOB in PGDA:PC:EC (60:25:15 wt) electrolyte compared to the reference electrolyte LP40.

In conclusion, this study highlights the potential of PGDA-based electrolytes, particularly when paired with thermally stable salts like LiBOB, to enable safer and more thermally robust lithium-ion cells.

Acknowledgments

This research was funded by the Bundesministerium für Wirtschaft und Energie within the Klebbatterie - Entwicklung einer Festkörperbatterie auf Basis eines aufgesprühten klebenden Elektrolyten project (03EI6102C).

The authors thank Münster Electrochemical Energy Technology for providing the NCM622 electrode material and Varta AG for providing the graphite electrode material.

Author Contributions

Conceptualization: L.K. and K.P.B; methodology: L.K., M.S., C. Z. and K.P.B.; investigation: L.K. and P.F.; writing - original draft preparation: L.K. and M.S.; writing - review and editing: P.F., C.Z. and K.P.B.; visualization: L.K.; supervision: K.P.B.; project administration: L.K.; funding acquisition: K.P.B. All authors have read and agreed to the published version of the manuscript.

ORCID

Larissa Kiefer https://orcid.org/0009-0007-7285-8902
Marco Ströbel https://orcid.org/0000-0002-5921-8747
Philipp Finster https://orcid.org/0009-0009-0923-2506
Carlos Ziebert https://orcid.org/0000-0003-3034-7550
Kai Peter Birke https://orcid.org/0000-0002-9679-2369

References

1. A. Yoshino, K. Sanechika, and T. Nakajima, *Secondary battery*, United States Patent4,668,595 (1987).
2. A. Yoshino, *Angew. Chem. Int. Ed.*, **51**, 5798 (2012).
3. M. Liu, Z. Zeng, Y. Wu, W. Zhong, S. Lei, S. Cheng, J. Wen, and J. Xie, *Energy Storage Materials*, **65**, 103133 (2024).
4. K. Xu, *Chem. Rev.*, **114**, 11503 (2014).
5. Y. Nishi, *The Electrochemical Society Interface*, **25**, 71 (2016).
6. R. Spotnitz and J. Franklin, *Journal of Power Sources*, **113**, 81 (2003).
7. M. Richard and J. Dahn, *J. Electrochem. Soc.*, **146**, 2068 (1999).
8. X. Feng, M. Fang, X. He, M. Ouyang, L. Lu, H. Wang, and M. Zhang, *Journal of Power Sources*, **255**, 294 (2014).
9. L. Feng, L. Jiang, J. Liu, Z. Wang, Z. Wei, and Q. Wang, *Journal of Power Sources*, **507**, 230262 (2021).
10. X. Feng, M. Ouyang, X. Liu, L. Lu, Y. Xia, and X. He, *Energy Storage Materials*, **10**, 246 (2018).

11. Y. Wang, X. Feng, W. Huang, X. He, L. Wang, and M. Ouyang, *Adv. Energy Mater.*, **13**, 2203841 (2023).
12. B. Lei, W. Zhao, C. Ziebert, N. Uhlmann, M. Rohde, and H. J. Seifert, *Batteries*, **3**, 14 (2017).
13. F. Larsson, P. Andersson, P. Blomqvist, A. Lorén, and B.-E. Mellander, *Journal of Power Sources*, **271**, 414 (2014).
14. G. Kim, S. Jeong, M. Joost, E. Rocca, M. Winter, S. Passerini, and A. Balducci, *Journal of Power Sources*, **196**, 2187 (2011).
15. A. Tsurumaki, M. Agostini, R. Poiana, L. Lombardo, E. Lufrano, C. Simari, A. Matic, I. Nicotera, S. Panero, and M. A. Navarra, *Electrochimica Acta*, **316**, 1 (2019).
16. M. Sun, Z. Zeng, W. Zhong, Z. Han, L. Peng, S. Cheng, and J. Xie, *Batteries & Supercaps*, **5**, e202200338 (2022).
17. Z. Zeng, X. Chen, M. Sun, Z. Jiang, W. Hu, C. Yu, S. Cheng, and J. Xie, *Nano Lett.*, **21**, 3611 (2021).
18. L. Peng, C. Yu, Z. Zhang, R. Xu, M. Sun, L. Zhang, S. Cheng, and J. Xie, *Energy & Environmental Materials*, **6**, e12308 (2023).
19. L. Peng, C. Yu, S. Cheng, and J. Xie, *Batteries & Supercaps*, **6**, e202200553 (2023).
20. G. G. Eshetu, S. Grugeon, S. Laruelle, S. Boyanov, A. Lecocq, J.-P. Bertrand, and G. Marlair, *Phys. Chem. Chem. Phys.*, **15**, 9145 (2013).
21. MERCK KGaA, *Propylene Glycol diacetate, CAS Number 623-84-7; Darmstadt, Germany* (2022).
22. S. Hess, M. Wohlfahrt-Mehrens, and M. Wachtler, *J. Electrochem. Soc.*, **162**, A3084 (2015).
23. P. Kurzweil and O. K. Dietlmeier, *Elektrochemische Speicher* (Springer, Berlin) (2018).
24. M. Sterner and I. Stadler, *Energiespeicher-bedarf, Technologien, Integration* (Springer-Verlag, Berlin) (2017).
25. S. Ohneseit, P. Finster, C. Floras, N. Lubenau, N. Uhlmann, H. J. Seifert, and C. Ziebert, *Batteries*, **9**, 237 (2023).
26. A. Hofmann, M. Migeot, E. Thißen, M. Schulz, R. Heinzmann, S. Indris, T. Bergfeldt, B. Lei, C. Ziebert, and T. Hanemann, *ChemSusChem*, **8**, 1892 (2015).
27. I. U. Mohsin, C. Ziebert, M. Rohde, and H. J. Seifert, *J. Electrochem. Soc.*, **168**, 050544 (2021).
28. C. Ziebert, A. Melcher, B. Lei, W. Zhao, M. Rohde, and H. Seifert, "Electrochemical–thermal characterization and thermal modeling for batteries." *Emerging Nanotechnologies in Rechargeable Energy Storage Systems* (Elsevier, Amsterdam)195 (2017).
29. Y.-P. Yang, A.-C. Huang, Y. Tang, Y.-C. Liu, Z.-H. Wu, H.-L. Zhou, Z.-P. Li, C.-M. Shu, J.-C. Jiang, and Z.-X. Xing, *Polymers*, **13**, 707 (2021).
30. B.-T. Yu, W.-H. Qiu, F.-S. Li, and L. Cheng, *Journal of Power Sources*, **166**, 499 (2007).
31. G. Maier et al., *ATZextra*, **25**, 26 (2020).